Scaling of pre-equilibrium dilepton production in QCD Kinetic Theory

Oscar Garcia-Montero,^{1,*} Philip Plaschke,^{1,†} and Sören Schlichting^{1,‡}

¹Fakultät für Physik, Universität Bielefeld, D-33615 Bielefeld, Germany

(Dated: February 19, 2025)

We use QCD kinetic theory to compute dilepton production coming from the pre-equilibrium phase of the Quark-Gluon Plasma created in high-energy heavy-ion collisions. We demonstrate that the dilepton spectrum exhibits a simple scaling in terms of the specific shear viscosity η/s and entropy density $dS/d\zeta \sim (T\tau^{1/3})^{3/2}$, which can be derived from dimensional analysis in the presence of a pre-equilibrium attractor. Based on this scaling we perform event-by-event calculations of in-medium dilepton production and determine the invariant mass range where the pre-equilibrium yield is the leading contribution.

I. INTRODUCTION.

Developing a first principles understanding of the nonequilibrium QCD processes that lead to the formation of a close to equilibrium Quark-Gluon Plasma (QGP), is one of the most outstanding challenges in modern heavyion physics. By now it has been established [1, 2] that - in various different microscopic theories - the onset of hydrodynamic behavior typically occurs on the time scale of a single equilibrium relaxation time $\sim (4\pi\eta/s)/T_{\rm eq}$, as determined by the specific shear viscosity η/s and (local) temperature of the system. Over the course of this evolution, the non-equilibrium QGP also undergoes a rapid information loss, whereby (some) details of the initial conditions become irrelevant, such that the pre-equilibrium evolution is governed by pre-equilibrium attractors (see Ref. [3–8] and references therein) even before a viscous fluid dynamic description becomes applicable.

Despite significant theoretical progress, experimental measurements to probe the early-time pre-equilibrium dynamics of the QGP at present and future facilities at RHIC and the LHC remain elusive. Electromagnetic probes, namely photons (γ) and dileptons (l^+l^-) , provide promising candidates, as they are produced throughout the entire space-time evolution of the collisions, and due to the lack of re-interactions with the QGP medium, escape the reaction unscathed. However, experimental measurement that isolate this signal are extremely challenging, as in addition to the "direct" production, which can be further sub-divided into prompt contributions (Drell-Yan [9]), thermal photons/dileptons and early-time pre-equilibrium radiation of the QGP, photons and dileptons are also copiously produced from late stage hadronic decays (see e.g. [10, 11] and references therein).

Evidently, an important property of dileptons is the invariant mass M of the lepton pair, as it can be used to discriminate between different production mechanism [12, 13]. Generally speaking, lepton pairs with larger invariant masses tend to be produced at earlier

times, such that e.g. the Drell-Yan process is the main source of high-M dileptons. The intermediate mass region is produced by in-medium dileptons coming from the pre-equilibrium and thermal phase of the QGP. Recent estimates of the pre-equilibrium dilepton production have shown that in an invariant mass range of $3~{\rm GeV} < M < 4~{\rm GeV}$ the pre-equilibrium contribution can indeed exceed the thermal QGP and Drell-Yan contributions [13, 14], and first ideas to develop a phenomenology of the pre-equilibrium phase based on dilepton measurements have been developed [12, 15].

In this work we show that the pre-equilibrium dilepton production exhibits a simple scaling behavior (c.f. Eq. (5)) in terms of the specific shear viscosity η/s and local entropy density $dS/d^2\mathbf{x}_Td\zeta$ of the QGP, which can also be extended to other probes of the early preequilibrium phase [16]. By performing microscopic calculations in QCD kinetic theory (KT) [17–20], which simultaneously provides a consistent theoretical description of the thermalization of the QGP and the production of electromagnetic probes, we explicitly verify this scaling and compute the associated scaling function for the invariant mass spectrum $dN_{l+l-}/d^2\mathbf{x}_T M dM dy_Q$ of pre-equilibrium dileptons. Since the scaling allows for a particularly efficient implementation of pre-equilibrium dilepton production, we further perform state-of-the art phenomenological calculations of (direct) dilepton production in heavy-ion collisions, which demonstrate the importance of event-by-event fluctuations in determining the dilepton yield in the intermediate mass range 3 GeV < M < 4 GeV, where the pre-equilibrium production dominates.

II. PRE-EQUILIBRIUM DILEPTON PRODUCTION

Dilepton production in leading order QCD kinetic theory is governed by quark anti-quark annihilation, with the corresponding production rate determined by

$$\frac{dN_{l^+l^-}}{d^4Xd^4Q} = \frac{8\pi}{3}N_c \sum_f q_f^2 \alpha_{EM}^2 \int \frac{d^3p_1}{(2\pi)^3 p_1} \frac{d^3p_2}{(2\pi)^3 p_2} \times f_{q_f}(x, P_1) f_{\overline{q}_f}(x, P_2) \delta^{(4)}(Q - P_1 - P_2), \quad (1)$$

^{*} garcia@physik.uni-bielefeld.de

[†] pplaschke@physik.uni-bielefeld.de

[‡] sschlichting@physik.uni-bielefeld.de

where $Q = P_{l^+} + P_{l^-}$ is the four momentum of the dilepton pair. Over the short course of the pre-equilibrium phase, the space-time evolution of the non-equilibrium QGP can be locally described in terms of a Bjorken flow, such that the space-time differential is given by $d^4X = \tau d\tau d\zeta d^2\mathbf{x}_T$ where $\tau = \sqrt{t^2 - z^2}$ is the proper time, $\zeta = \operatorname{arctanh}(z/t)$ is the space-time rapidity and \mathbf{x}_T denotes the transverse coordinates. While in thermal equilibrium, the production rate can be integrated to yield the well known leading order result (see also [21, 22] for NLO corrections)

$$\frac{dN_{l^+l^-}}{d^4Xd^4Q} = \frac{N_C\alpha_{\rm EM}^2}{12\pi^4} \sum_f q_f^2 \frac{F(q)}{\exp(q^0/T) - 1} \,, \eqno(2)$$

with

$$F(q) = \frac{2T}{q} \ln \left[\cosh \left(\frac{q^0 + q}{4T} \right) / \cosh \left(\frac{q^0 - q}{4T} \right) \right]$$
(3)

the non-equilibrium production of dilepton pairs is governed by the phase-space distributions of quarks and antiquarks $f_{q_f}(x, P_1)$ and $f_{\overline{q}_f}(x, P_2)$ in Eq. (1).

During the pre-equilibrium phase the QGP is believed to be highly anisotropic in momentum space, as it is subject to a rapid longitudinal expansion, and dominated by gluon degrees a freedom, as these are more copiously produced in the initial (semi-) hard scatterings [2, 23]. Notably, these effects result in a momentumspace anisotropy [24, 25], a non-trivial polarization [12] and an overall suppression of the dilepton yield, as discussed in previous works [12–14], where a phenomenological parametrization of the phase-space distributions $f_{q/\bar{q}}$ was employed to compute the pre-equilibrium dilepton production. Conversely, in this work we will compute the pre-equilibrium dilepton production directly from a microscopic calculation in QCD kinetic theory, following the procedure we have presented in Refs. [16]. However, before we present results of our microscopic calculations, it proves particularly insightful to perform a dimensional scaling analysis of the pre-equilibrium dilepton yield.

A. Scaling of pre-equilibrium dilepton production

Generally, the pre-equilibrium production of electromagnetic probes will proceed differently at different positions \mathbf{x}_T in the transverse plane and depend on the timescale $\tau_{\rm eq}(\mathbf{x}_T)$, and the temperature $T_{\rm eq}(\mathbf{x}_T)$ at which the system locally approaches a viscous hydrodynamic description. By dimensional analysis, it is natural to assume, that the local production rate $\frac{dN_{l+l-}}{d^4Xd^4Q}$ at each transverse position \mathbf{x}_T only depends on the dimensionless ratios $\tau/\tau_{\rm eq}(\mathbf{x}_T)$ and $Q/T_{\rm eq}(\mathbf{x}_T)$,

$$\frac{dN_{l^+l^-}}{d^4Xd^4Q} = \frac{dN_{l^+l^-}}{d^4Xd^4Q} \left(\frac{\tau}{\tau_{\rm eq}(\mathbf{x}_T)}, \frac{Q}{T_{\rm eq}(\mathbf{x}_T)}\right)$$
(4)

such that upon integrating over the production time τ , the space-time time rapidity ζ , and the transverse

momentum q_T of the dilepton pair, the local yield $\frac{dN_{l^+l^-}}{d^2\mathbf{x}_TMdMdy_Q} = \int d\tau \tau \int d\zeta \int d^2q_T \frac{dN_{l^+l^-}}{d^4Xd^4Q}$ per unit rapidity y_Q and invariant mass $M = \sqrt{Q^2}$ is determined by

$$\frac{dN_{l^+l^-}}{d^2\mathbf{x}_T M dM dy_Q} = \tau_{\text{eq}}^2(\mathbf{x}_T) T_{\text{eq}}^2(\mathbf{x}_T) \, \mathcal{N}_{l^+l^-} \left(\frac{M}{T_{\text{eq}}}\right) \tag{5}$$

where $N_{l^+l^-}$ is a scaling function, which only depends on the ratio M/T_{eq} , and is determined by

$$\mathcal{N}_{l^+l^-} \left(\frac{M}{T_{\text{eq}}} \right) = \int d\frac{\tau}{\tau_{\text{eq}}} \frac{\tau}{\tau_{\text{eq}}} \int d\zeta \int d^2 \frac{q_T}{T_{\text{eq}}}$$

$$\frac{dN_{l^+l^-}}{d^4 X d^4 Q} \left(\frac{\tau}{\tau_{\text{eq}}}, \frac{Q}{T_{\text{eq}}} \right)$$
(6)

While the calculation of the scaling function $\mathcal{N}_{l^+l^-}\left(\frac{M}{T_{\rm eq}}\right)$ is highly non-trivial, it is comparatively straightforward to isolate the dependence on the local entropy density and coupling strength of the system. We first note that different studies at weak [26, 27] and strong coupling [4, 5, 8]) indicate, that equilibration of the out-of-equilibrium QGP is controlled by the equilibrium relaxation rate $\Gamma_{\rm eq} = T_{\rm eq}/(4\pi\eta/s)$, such that hydrodynamics becomes applicable when the dimensionless scaling variable $\tilde{w} = \Gamma_{\rm eq} \tau_{\rm eq}$ is of order unity, such that

$$\tau_{\rm eq} T_{\rm eq} \approx 4\pi \eta / s \,.$$
 (8)

Since the equilibrium temperature $T_{\rm eq}$ can be related to the local entropy density of the system $\frac{dS}{d^2\mathbf{x}_Td\zeta}$, which in turn is directly related to the multiplicity of charged particles produced in the collisions, one further obtains the relation

$$\frac{2\pi^2}{45}\nu_{\text{eff}}\tau_{\text{eq}}T_{\text{eq}}^3 \approx \frac{dS}{d^2\mathbf{x}_T d\zeta} \tag{9}$$

where $\nu_{\rm eff} \approx 32$ denotes the effective number of bosonic degrees of freedom [28, 29]. Denoting the dependence on the local entropy density in terms of the quantity $(T\tau^{\frac{1}{3}})_{\infty}^{3/2} = \sqrt{\frac{dS}{d^2\mathbf{x}_T d\zeta}/\left(\frac{2\pi^2}{45}\nu_{\rm eff}\right)}$, by virtue of Eqns. (8) and (9) the equilibration time and equilibration temperature can then be determined as

$$\tau_{\rm eg} \approx (T\tau^{\frac{1}{3}})_{\infty}^{-3/2} (4\pi\eta/s)^{3/2}$$
 (10)

$$T_{\rm eq} \approx (T\tau^{\frac{1}{3}})_{\infty}^{3/2} (4\pi\eta/s)^{-1/2}$$
 (11)

and the pre-equilibrium dilepton yield can be expressed as

$$\frac{dN_{l^+l^-}}{d^2\mathbf{x}_T M dM dy_Q} = (4\pi\eta/s)^2 \, \mathcal{N}_{l^+l^-} \left(\frac{\sqrt{4\pi\eta/s} \, M}{(T\tau^{1/3})_{\infty}^{3/2}} \right) \quad (12)$$

Strikingly, the above scaling can be derived on rather general grounds, and thus easily extended to a variety of

other quantities, such as e.g. the transverse momentum (q_T) spectrum, which takes the form

$$\frac{dN_{l^+l^-}}{d^2\mathbf{x}_T d^2\mathbf{q}_T M dM dy_O} = (4\pi\eta/s)^3 (T\tau^{\frac{1}{3}})_{\infty}^{-3}$$
(13)

$$\mathcal{N}_{l^+l^-} \left(\frac{\sqrt{4\pi\eta/s} \ M}{(T\tau^{\frac{1}{3}})_{\infty}^{3/2}}, \frac{\sqrt{4\pi\eta/s} \ q_T}{(T\tau^{\frac{1}{3}})_{\infty}^{3/2}} \right)$$
 (14)

Most importantly, such scaling can also be expected to be present for other processes, such as e.g. the pre-equilibrium production of photons [16], heavy flavor quarks [30] or pre-equilibrium jet quenching [31], which will greatly facilitate their phenomenological treatment in the future.

B. Dilepton production from non-equilibrium QGP evolution.

In order to verify the predicted scaling we compute the pre-equilibrium spectrum of dileptons for different values of the coupling $\lambda = 4\pi N_c \alpha_s$ using a QCD kinetic theory description, where we incorporate all leading order processes of quarks and gluons into the Boltzmann equation to compute the respective distribution functions during the pre-equilibrium evolution of the QGP [16, 18, 27]. Within this framework infrared divergencies are regulated by an isotropic screening [26, 27, 32-34] and in-medium effects associated with the Landau-Pomeranchuk-Migdal (LPM) effect are treated via an effective vertex resummation. Starting from a gluon dominated initial state as in [16], we numerically solve the Boltzmann equation to determine the evolution of the phase-space distributions $f_{q/\overline{q}}$, which then enables us to compute the dilepton rate at each time step. The procedure for the evolution of the pre-equilibrium QGP, which serves as a background to the dilepton production rate, Eq. (1), was described in Ref. [16]. For the numerical computation of the dilepton rate we use the same setup as in the aforementioned photon production study, including the same initial conditions and the assumption of boost invariance.

Since the QGP created in relativistic heavy-ion collisions at RHIC and LHC energies remains strongly coupled, as indicated by a small shear-viscosity to entropy density ratio η/s , the framework of QCD Kinetic Theory is not directly applicable and the results need to be extrapolated to realistic coupling strength for phenomenological application. In this context, it is important to point out that studies of the pre-equilibrium evolution in various weakly [7, 32, 35, 36] and strongly coupled theories [37, 38] indicate that the processes of kinetic and chemical equilibration are governed by a single timescale related to the equilibrium relaxation time τ_R , determined by the shear viscosity to entropy density ratio [39]. While we use weakly-coupled QCD Kinetic Theory to calculate the pre-equilibrium evolution of the

λ	5	10	20
	0.133		
	2.716		
$(\tau^{1/3}T)_{\infty}/Q_s^{2/3}$	0.799	0.612	0.474

Table I. Strong coupling α_s , shear viscosity to entropy density ratio η/s and asymptotic temperature $(\tau^{1/3}T)_{\infty}/Q_s^2$ for different coupling strengths λ .

phase-space distributions of quarks and gluons, we therefore anticipate that the non-equilibrium effects of the bulk anisotropy and gluon dominance on dilepton production can be considered representative of different microscopic models. Therefore, we also anticipate that the results can be extrapolated to viable coupling strength based on the scaling variables $\tilde{w} \approx \tau T_{\rm eff}(\tau)/4\pi\eta/s$, and $(\eta/s)^{1/2}M/(\tau^{1/3}T)_{\infty}^{3/2}$; showing weak dependence on coupling strength and consistent behavior across different microscopic models.

Numerical results for the pre-equilibrium spectrum of dileptons as a function of invariant mass are presented in Fig. 1a, where we show the integrated dilepton yield up to $\tilde{w} = 0.5$ (top), during the thermalization process of the QGP and 1.0 (bottom), when visc. hydrodynamics becomes applicable. When comparing the results for different coupling strength $\lambda = 5, 10, 20$, which correspond to different values of the specific shear viscosity η/s , we express the spectra in terms of the invariant mass $M/(\tau^{1/3}T)_{\infty}^{3/2}$ (in Fig. 1a) and the re-scaled invariant mass variable $(\eta/s)^{1/2}M/(\tau^{1/3}T)_{\infty}^{3/2}$ (in Fig. 1b). The specific shear viscosity as well as the asymptotic constant $(\tau^{1/3}T)_{\infty}$ are obtained by comparison to the first order viscous hydrodynamic expansions of the longitudinal pressure resp. the effective temperature (see [16, 33, 40] for more details). The results for $\lambda = 5, 10, 20$ are compactly summarized in Table I.

Thus, variations in the coupling reflect the sensitivity of this scaling parameter, as illustrated in Fig. 1.

When comparing the results for different coupling strength as a function of $M/(\tau^{1/3}T)_\infty^{3/2}$, we see that stronger couplings tend to produce more large-M dileptons. Setting $(\tau^{1/3}T)_\infty^{3/2}=0.402$ GeV as in [16], to mimic the conditions in central Pb+Pb collisions at LHC energies, this occurs for invariant masses $M\gtrsim 2$ GeV. Below $M\lesssim 2$ GeV this changes and more weakly coupled systems produce more dileptons during the pre-equilibrium phase, i.e. for $\tilde{w}<1$. We further see that high-M dileptons are predominantly produced at the earliest times of the evolution. Indeed, the curves for $\tilde{w}=0.5$ are almost not modified during the evolution up to $\tilde{w}=1.0$. However, in the mean time the QGP produces many low-mass dileptons, such that the spectrum increases significantly in the low-M regime.

Besides the QCD kinetic theory results, we also show results for an effective parameterization (EP) of the distribution functions already used in previous works for pre-equilibrium dilepton production [12–14], where the

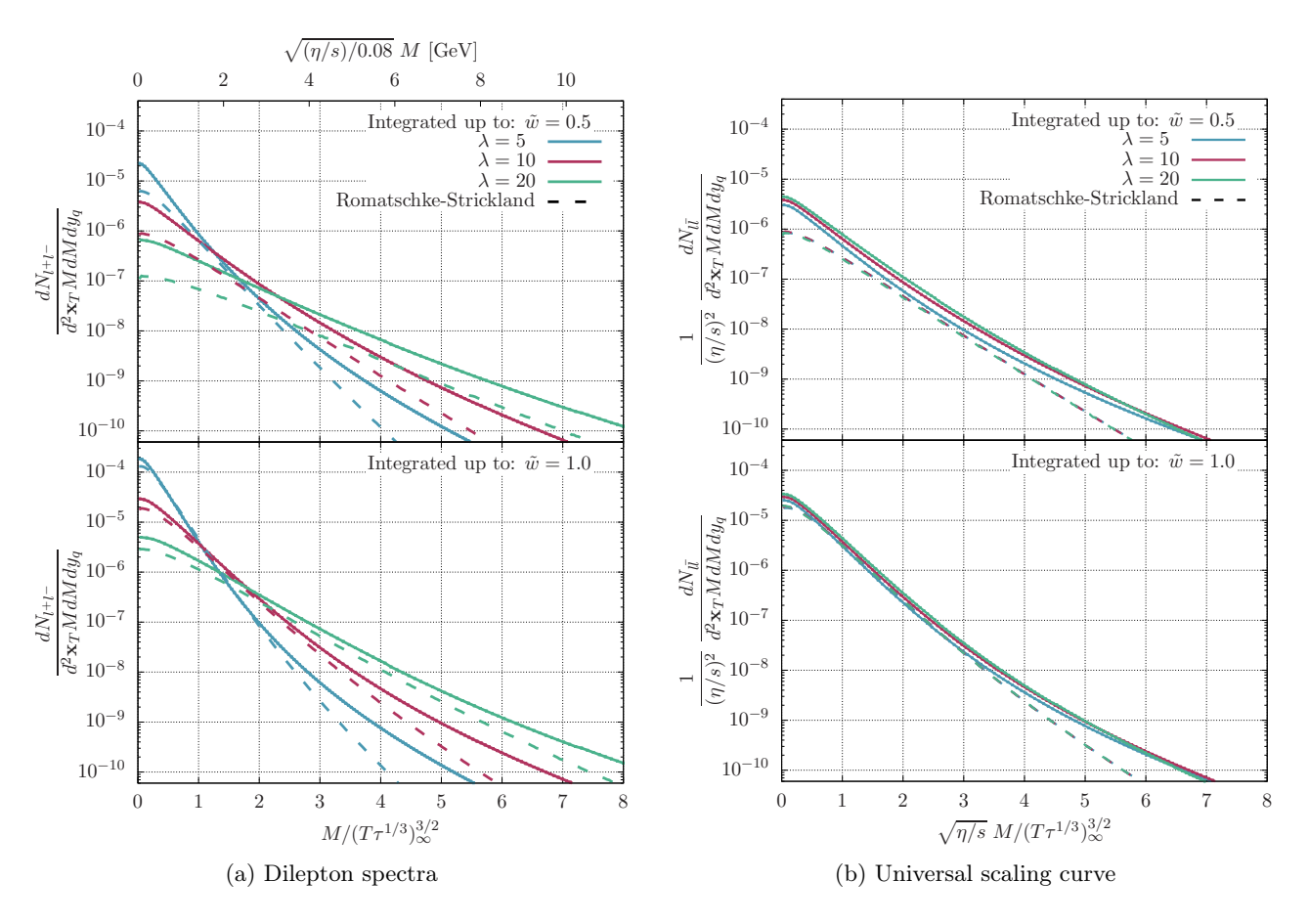


Figure 1. Spectrum of dileptons produced during the pre-equilibrium stage as a function of (a) $M/(T\tau^{1/3})_{\infty}^{3/2}$ and (b) $\sqrt{\eta/s}M/(T\tau^{1/3})_{\infty}^{3/2}$. Different colors correspond to different coupling strengths $\lambda = 5, 10, 20$ and different panels correspond to different final integration times $\tilde{w} = 0.5, 1.0$. Spectra in the right panels are divided by $(\eta/s)^2$ in order to obtain the universal scaling curve.

authors used anisotropic equilibrium distribution functions of the Romatschke-Strickland form (see Fig 1b and Ref. [41]), together with an overall quark suppression factor. Compared to the QCD KT results, the spectra computed from the effective parameterization are suppressed at both times, although the suppression is stronger for earlier times. This is expected as the description of pre-equilibrium dynamics in terms of anisotropic equilibrium distributions is worse for earlier time dynamics. Over the course of the evolution, the spectra for the effective parametrization get closer to the QCD KT results and for smaller couplings we find almost the same spectra for the low and intermediate mass range.

To verify the universal scaling, we re-plot the same spectra in Fig. 1b with the predicted scaling from Eq. (12). By construction, the spectra obtained using the effective parametrization perfectly collapse to each other, while the QCD KT results also get much closer to each other. Since the scaling function $N_{l^+l^-}$ is derived on basis of an attractor solution, the scaling for the QCD KT results works better and better for later evolution. Especially for $\tilde{w} \gtrsim 1$, which is in accordance with the

hydrodynamization time found in earlier studies in the context of QCD kinetic theory [7, 33, 35, 36], the scaling works very well, whereas at very early times the spectra are sensitive to the initial conditions for the kinetic evolution. We discuss the residual deviations from scaling further in Appendix A.

III. PHENOMENOLOGY OF THE PRE-EQUILIBRIUM DILEPTON PRODUCTION

One remarkable consequence of the scaling formula is the practical usage for phenomenological calculations and comparisons to experimental data. In order to demonstrate this, we match the QCD KT evolution to the initial conditions of the subsequent hydrodynamic evolution of the QGP. By use of the scaling formula in Eq. 12, the only other ingredients to compute the spectrum of dileptons produced during the pre-equilibrium are the (local) temperature $T(\tau_{\text{hydro}}, \mathbf{x}_T) \equiv T_{\text{hydro}}(\mathbf{x}_T)$ at initialization time τ_{hydro} and the specific shear-viscosity η/s . Based on this information, the local values of the scaling variable

 $\tilde{w}(\mathbf{x}_T)$ can then be determined as

$$\tilde{w}(\mathbf{x}_T) = \frac{\tau_{\text{hydro}} T_{\text{hydro}}(\mathbf{x}_T)}{4\pi \eta / s}, \qquad (15)$$

and similarly, the energy scale $(\tau^{1/3}T)_{\infty}(\mathbf{x}_T)$ can be obtained according to [33, 40]

$$(\tau^{1/3}T)_{\infty}(\mathbf{x}_T) = \tau_{\text{hydro}}^{1/3} \left(T_{\text{hydro}}(\mathbf{x}_T) + \frac{2}{3} \frac{\eta/s}{\tau_{\text{hydro}}} \right)$$
 (16)

accounting for first order viscous corrections. Once those two quantities are determined at each point in the transverse plane, the total pre-equilibrium dilepton yield is then given by

$$\frac{dN_{l^+l^-}}{MdMdy_Q} = (4\pi\eta/s)^2 \int d^2\mathbf{x}_T \, \mathcal{N}_{l^+l^-} \left(\tilde{w}(\mathbf{x}_T), \frac{\sqrt{\eta/s} \, M}{(T\tau^{1/3})_{\infty}^{3/2}(\mathbf{x}_T)} \right). \tag{17}$$

We compute the event-by-event dilepton spectra at midrapidity for Pb-Pb collisions at $\sqrt{s_{NN}} = 5.02$ TeV. To account for a background evolution well fit to data, we created the events using the hybrid model Trajectum [42], and used one of the consistent parameter sets extracted using the Bayesian analysis in Ref. [43]. We focus on the 0-5% class, and obtain the pre-equilibrium dilepton yield by integrating event-by-event over the initial profiles for the hydrodynamical evolution as in Eq. (17). By matching the initial profiles to the subsequent hydrodynamic evolution at $\tau_{hydro} = 1.0$ fm as in [16], the thermal QGP contribution is then found by folding the thermal dilepton production rate with the background hydrodynamic evolution from $\tau_{hydro} = 1.0$ fm onwards¹. Clearly, one of the main advantages of using this description is that it guarantees for a smooth matching between pre-equilibrium and hydrodynamical dilepton production, such that the overall spectrum of in-medium dileptons is rather insensitive to the matching time τ_{hydro} , as discussed further in Appendix A.

We present our main phenomenological result in Fig. 2, where we compare the in-medium dilepton production, to the Drell-Yan (DY) contribution, computed to NLO precision with the EPPS nPDFs [44] by using the DYTurbo software [45], where as in previous works [13] the centrality dependence of the nPDFs was neglected and T_{AA} scaling was assumed. While the top panel of Fig. 2 shows the total dilepton yield $dN_{l^+l^-}/dMdy_Q$, the lower panel shows a break-up of the total yield into DY and thermal QGP contributions, as well as in the the pre-equilibrium contribution from ranges of evolution time \tilde{w} , and clearly

illustrates how larger invariant masses correspond to earlier production times.

While at higher invariant mass ranges the DY contribution is well constrained and therefore presents small uncertainties, at low Ms, it presents large error bands, due to large scale uncertainties. Despite these large theoretical uncertainties, we find that the pre-equilibrium dilepton contribution obtained from realistic event-by-event QCD KT+Hydro simulations dominates over both the DY and thermal QGP background for invariant masses $\sim 3~{\rm GeV}$.

Beyond the results obtained from event-by-event (EBvE) simulations, we have also computed the inmedium dilepton spectra for a coarse grained (CG) description, where similar to [46, 47] we compute the emission for a single average event, as well as comparing to previous obtained results for a simple Bjorken scaling scenario [13], where transverse dynamics of the QGP is completely neglected. While the Bjorken scaling underestimates the cooling of the QGP, and thus overestimates the dilepton yield by almost a factor of three, the coarse grained averaged description provides a very good description for low invariant masses ≤ 2 GeV. Nevertheless, the coarse grained description also but underestimates the high M tails of in-medium dilepton production, which are more likely produced from local hot spots, and we therefore conclude from this analysis, that an event-byevent description is desirable to provide accurate predictions for high and intermediate mass dileptons. This difference between the EbE and CG descriptions becomes more important for less central collisions.

We close our discussion by putting our calculations of pre-equilibrium dilepton production in the context of other recent works, discussing the most important similiarities and differences in methodology and findings. While our studies are based on event-by-event calculations with microscopic non-equilibrium rates, a number of works have addressed the same question of using dileptons as probes to extract information about the early stages, following the interest to address the same question using real photons [16, 48–51].

In [13, 14], the authors estimate the relative contributions of the in-medium production (pre-equilibrium and hydro stages) with respect to the expected Drell-Yan contribution and find that there is a window $M \approx 2-3.5$ GeV in which the pre-equilibrium dominates. In this estimate, the authors consider a transversely homogeneous system undergoing a simple Bjorken expansion (as in our transversely homogenous scenario), and the non-equilibrium dilepton rates are determined from a QCD KT inspired parametrization of the phase-space distribution of quarks and gluons (as in our Romatsche-Strickland paramtrization). Even though the Bjorken scenario may lead to a slight overestimation of the pre-equilibrium dilepton rate, the results of [13, 14] are generally consistent with our findings; moreover the authors also proposed the polarization of dilepton pairs as a possible means to discriminate between pre-equilibrium and Drell-Yan contri-

¹ The QGP rate is folded with the hydro evolution for temperatures higher than $T_c = 154$ MeV. Below this temperature, hadronic degrees of freedom dominate, and the rate can be computed from effective theories [42]. Nevertheless, the hadronic rates are too soft to contribute significantly to the invariant mass range relevant to this work.

butions [12] and it would be interesting to extend our methodology to such polarization observables.

In [52] the authors perform event-by-event studies of pre-equilibrium dilepton production. Based on the macroscopic pre-equilibrium evolution of the energymomentum tensor in KøMPøST [33, 35], the authors extract an effective temperature, which is then employed in thermal rates to compute the pre-equilibrium production. Non-equilibrium effects on the rates are accounted for by introducing a phenomenological quark suppression factor, inspired by Refs. [26, 53]. However, the authors do not take into account the modified shapes of the preequilbrium momentum distributions of quarks and gluons, (see. e.g. [16]), which is particularly relevant for the hardest part of the spectrum produced at the earliest times. Qualitatively, the results of [52] give a very similar picture for the expected mass spectrum of dileptons in ultra-relativistic HICs, albeit the calculation of [52] slighty overshoots our results. This gives a wider window of relevance for the measurement of pre-equilibrium dileptons.

IV. SUMMARY AND OUTLOOK.

We computed the pre-equilibrium spectrum of dileptons in QCD kinetic theory and showed that it exhibits a simple universal scaling in terms of the specific shear viscosity η/s and entropy density $(T\tau^{1/3})_{\infty}$. Such scaling functions are powerful tools as they allow for event-by-event calculations of the corresponding spectra by matching η/s and $(T\tau^{1/3})_{\infty}$ to realistic values of a heavy-ion collision. By performing realistic event-byevent simulations of pre-equilibrium, thermal QGP and Drell-Yan dilepton production for $\sqrt{s_{NN}} = 5.02$ TeV Pb-Pb collisions, we find that the pre-equilibrium production dominates over the irreducible background for invariant masses ~ 3 GeV. However, this result only serve as an illustrative example and in order to make full use of our results for phenomenological applications, we have included the pre-equilibrium scaling functions into the initial state framework KøMPøST. This version including photons and dileptons is called ShinyKøMPøST and is publicly available under [54].

Since the pre-equilibrium scaling in Eq. (12) can be derived on rather general grounds, it can also be extended to fully differential dilepton observables, which is highly beneficial for the development of a Monte-Carlo generator to facilitate the detection of pre-equilibrium dileptons in present and future heavy-ion experiments. Since earlier studies showed that the polarization of dileptons is a key observable to distinguish the pre-equilibrium emission from other sources [12], clearly a next step will be to derive analogous scaling functions for polarization observables. However, the use of pre-equilibrium scaling functions is by no means limited to electromagnetic probes, an extension to relevant topics such as heavy-flavor production [30, 55–57], heavy-quark diffusion [58]

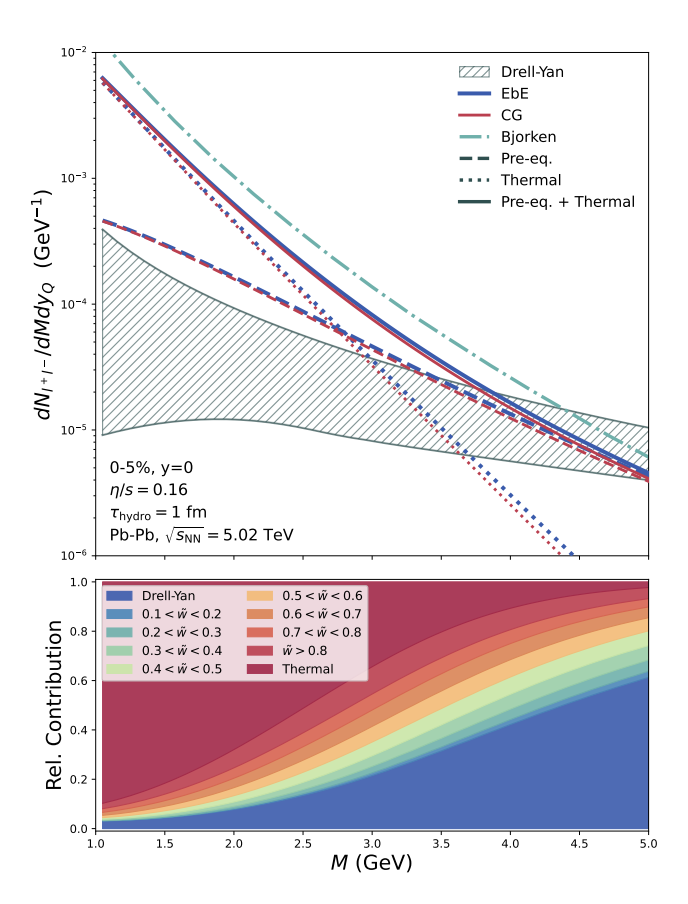


Figure 2. (Upper panel) Comparison of the in-medium dilepton spectrum for 0–5% centrality Pb-Pb collisions at $\sqrt{s_{NN}}$ = 5.02 TeV to their corresponding Drell-Yan contribution. The in-medium contributions are shown for three different cases (transversely homogeneous Bjorken expansion (data taken from [13]), realistic EbE ICs, and smooth initial conditions, the average of the latter). (Lower panel) Relative contribution of the different contributions to the total yield (in-medium + Drell-Yan). The EbE pre-equilibrium has been split into different \tilde{w} ranges for better comparison.

or jet energy loss [59] would be interesting to see and deserves further theoretical attention.

ACKNOWLEDGEMENTS

We thank Maurice Coquet, Travis Dore, Xiaojian Du, Stephan Ochsenfeld, Jean-Yves Ollitrault, Michael Winn for valuable discussions. The authors want to thank Aleksas Mazeliauskas for collaboration on related work. OGM, PP and SS acknowledge support by the Deutsche Forschungsgemeinschaft (DFG, German Research Foundation) through the CRC-TR 211 'Strong-interaction matter under extreme conditions'-project number 315477589 – TRR 211. OGM and SS acknowledge also support by the German Bundesministerium für Bildung und Forschung (BMBF) through Grant No. 05P21PBCAA. The authors acknowledge

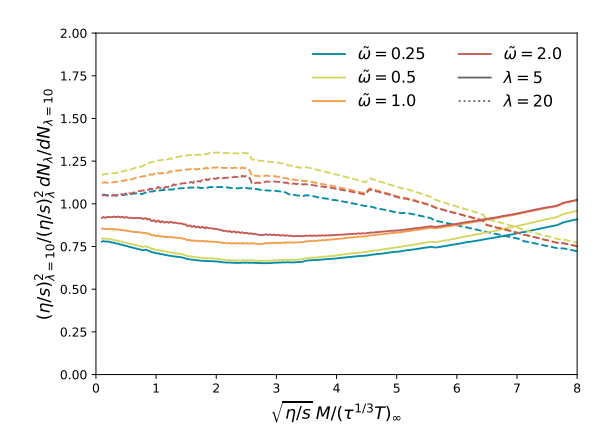


Figure 3. Scaling function comparison for different coupling constants ($\lambda=5,10,20$), normalized to $\lambda=10$. Deviations remain within 30–35% for relevant mass ranges and decrease to < 20% for $\tilde{w} \geq 1$, supporting the robustness of the scaling approach.

computing time provided by the Paderborn Center for Parallel Computing (PC2) and the National Energy Research Scientific Computing Center, a DOE Office of Science User Facility supported by the Office of Science of the U.S. Department of Energy under Contract No. DE-AC02-05CH11231.

Appendix A: Sensitivity of pre-equilibirum dilepton production on coupling constant (λ) and matching time $(\tau_{\rm Hyhdro})$

Below we discuss the dependence of the scaling function on the coupling constant λ , and the sensitivity of the integrated dilepton yield on the matching time, $\tau_{\rm hydro}$.

1. Sensitivity of the coupling constant, λ

By virtue of the scaling functions, the leading coupling dependence of the integrated yields is taken into account. While, by construction, this scaling is exact for the Romatschke-Strickland form of the phase-space distributions, the scaling relations Eq. (12) are only approximate for EKT, and it is thus important to assess residual deviations from scaling

In Fig. 3, we have included a comparison of the resulting scaling function for the choice of three different coupling constants. This is presented as the ratio of the extremal values, $\lambda = (5,20)$, normalized by the scaling function for the choice of $\lambda = 10$. For the phenomenologically relevant values of the rescaled invariant mass, the scaling holds down to deviations no larger than 30-35%. However, it is important to emphasize that for large $\tilde{\omega}$, where the phase-space distributions in EKT become more and more similar to the Romatsche-Strickland form, de-

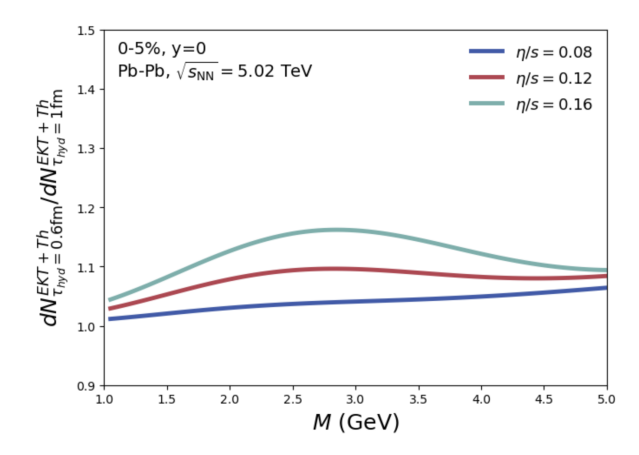


Figure 4. Effect of hydrodynamization time $\tau_{\rm hydro}$ on dilepton production. The ratio of spectra for $\tau_{\rm hydro} = 0.6$ and 1.0 fm shows up to 20% variation, with larger deviations for higher shear viscosity.

viations get smaller and smaller, such that already for $\tilde{\omega} = 1$ we find that deviations are no larger than 20%.

Since the phenomenological application of the scaling formula only makes sense in the cases where the kinetic system has already effectively thermalized, the switching to thermal production has to be performed around $\tilde{\omega} \gtrapprox 1$, we consider this level of accuracy sufficient for phenomenological applications.

2. Sensitivity to the matching time $\tau_{\rm hydro}$

By following our procedure in Ref. [16], we have studied how changes in the switching time, τ_{hydro} , affect the overall invariant mass spectrum of dileptons. In a idealized setup, where the simulation is perfectly matched between the early non-equilibrium thermalization process and the ensuing hydro stage, one would expect that the overall dilepton spectra should be independent to the switching time. The reason for this is naturally that the pre-equilibrium stage flows smoothly into the hydrodynamical – close-to-equilibrium – stage. Nevertheless, in all state-of-the-art simulations there will be regions of the space-time evolution, like cells in the boundary of the fluid, which do not perfectly satisfy the matching condition $(\tilde{\omega} \geq 1)$. While we have checked that the average of the cells – weighted by energy – satisfies this condition, a large enough volume of fringe cells with $\tilde{\omega}_{\mathrm{matching}} < 1$ may reduce the overlap. The reason for this is the parametric dependences of $\tilde{\omega}$, where increasing the shear viscosity, while fixing $\tau_{\rm hydro}$ and the temperature of the matched cell, T_{hydro} , decreases the effective $\tilde{\omega}$, hence decreasing the overlap for smaller τ_{hydro} . In other words, the cell volume with $\tilde{\omega}_{\mathrm{matching}} < 1$ becomes larger for earlier times. We have quantified these effects in Fig. 4, where we plot the ratio of the total in-medium production spectrum (EKT+Hydro), for two

different mathing times, $\tau_{\text{hydro}} = [0.6, 1.0]$. We have observed that for larger shear viscosities, the matching is

less smooth. That being said, such effects seem to be no larger than 20% in magnitude for the systems studied in this work.

- S. Schlichting and D. Teaney, The First fm/c of Heavy-Ion Collisions, Ann. Rev. Nucl. Part. Sci. 69, 447 (2019), arXiv:1908.02113 [nucl-th].
- [2] J. Berges, M. P. Heller, A. Mazeliauskas, and R. Venugopalan, QCD thermalization: Ab initio approaches and interdisciplinary connections, Rev. Mod. Phys. 93, 035003 (2021), arXiv:2005.12299 [hep-th].
- [3] M. P. Heller and M. Spalinski, Hydrodynamics Beyond the Gradient Expansion: Resurgence and Resummation, Phys. Rev. Lett. **115**, 072501 (2015), arXiv:1503.07514 [hep-th].
- [4] W. Florkowski, M. P. Heller, and M. Spalinski, New theories of relativistic hydrodynamics in the LHC era, Rept. Prog. Phys. 81, 046001 (2018), arXiv:1707.02282 [hep-ph].
- [5] P. Romatschke and U. Romatschke, Relativistic Fluid Dynamics In and Out of Equilibrium, Cambridge Monographs on Mathematical Physics (Cambridge University Press, 2019) arXiv:1712.05815 [nucl-th].
- [6] A. Kurkela, W. van der Schee, U. A. Wiedemann, and B. Wu, Early- and Late-Time Behavior of Attractors in Heavy-Ion Collisions, Phys. Rev. Lett. 124, 102301 (2020), arXiv:1907.08101 [hep-ph].
- [7] X. Du and S. Schlichting, Equilibration of the Quark-Gluon Plasma at Finite Net-Baryon Density in QCD Kinetic Theory, Phys. Rev. Lett. 127, 122301 (2021), arXiv:2012.09068 [hep-ph].
- [8] A. Soloviev, Hydrodynamic attractors in heavy ion collisions: a review, Eur. Phys. J. C 82, 319 (2022), arXiv:2109.15081 [hep-th].
- [9] S. D. Drell and T.-M. Yan, Massive Lepton Pair Production in Hadron-Hadron Collisions at High-Energies, Phys. Rev. Lett. 25, 316 (1970), [Erratum: Phys.Rev.Lett. 25, 902 (1970)].
- [10] R. Rapp, Dilepton Spectroscopy of QCD Matter at Collider Energies, Adv. High Energy Phys. 2013, 148253 (2013), arXiv:1304.2309 [hep-ph].
- [11] G. Vujanovic, J.-F. Paquet, G. S. Denicol, M. Luzum, S. Jeon, and C. Gale, Electromagnetic radiation as a probe of the initial state and of viscous dynamics in relativistic nuclear collisions, Phys. Rev. C 94, 014904 (2016), arXiv:1602.01455 [nucl-th].
- [12] M. Coquet, X. Du, J.-Y. Ollitrault, S. Schlichting, and M. Winn, Dilepton polarization as a signature of plasma anisotropy, (2023), arXiv:2309.00555 [nucl-th].
- [13] M. Coquet, X. Du, J.-Y. Ollitrault, S. Schlichting, and M. Winn, Intermediate mass dileptons as pre-equilibrium probes in heavy ion collisions, Phys. Lett. B 821, 136626 (2021), arXiv:2104.07622 [nucl-th].
- [14] M. Coquet, X. Du, J.-Y. Ollitrault, S. Schlichting, and M. Winn, Transverse mass scaling of dilepton radiation off a quark-gluon plasma, Nucl. Phys. A 1030, 122579 (2023), arXiv:2112.13876 [nucl-th].
- [15] F. Seck, B. Friman, T. Galatyuk, H. van Hees, E. Speranza, R. Rapp, and J. Wambach, Polarization of Thermal Dilepton Radiation, (2023), arXiv:2309.03189 [nucl-th].

- [16] O. Garcia-Montero, A. Mazeliauskas, P. Plaschke, and S. Schlichting, Pre-equilibrium photons from the early stages of heavy-ion collisions, (2023), arXiv:2308.09747 [hep-ph].
- [17] P. B. Arnold, G. D. Moore, and L. G. Yaffe, Photon and gluon emission in relativistic plasmas, JHEP 06, 030, arXiv:hep-ph/0204343.
- [18] P. B. Arnold, G. D. Moore, and L. G. Yaffe, Effective kinetic theory for high temperature gauge theories, JHEP 01, 030, arXiv:hep-ph/0209353.
- [19] P. B. Arnold, G. D. Moore, and L. G. Yaffe, Photon emission from quark gluon plasma: Complete leading order results, JHEP 12, 009, arXiv:hep-ph/0111107.
- [20] P. B. Arnold, G. D. Moore, and L. G. Yaffe, Photon emission from ultrarelativistic plasmas, JHEP 11, 057, arXiv:hep-ph/0109064.
- [21] R. Baier, B. Pire, and D. Schiff, Dilepton production at finite temperature: Perturbative treatment at order α_s , Phys. Rev. D **38**, 2814 (1988).
- [22] J. Churchill, L. Du, C. Gale, G. Jackson, and S. Jeon, Dilepton production at NLO and intermediate invariantmass observables, (2023), arXiv:2311.06675 [nucl-th].
- [23] E. Iancu and R. Venugopalan, The Color glass condensate and high-energy scattering in QCD, in *Quark-gluon plasma 4*, edited by R. C. Hwa and X.-N. Wang (2003) pp. 249–3363, arXiv:hep-ph/0303204.
- [24] B. S. Kasmaei and M. Strickland, Dilepton production and elliptic flow from an anisotropic quark-gluon plasma, Phys. Rev. D 99, 034015 (2019), arXiv:1811.07486 [hepph].
- [25] B. S. Kasmaei and M. Strickland, Photon production and elliptic flow from a momentum-anisotropic quark-gluon plasma, Phys. Rev. D 102, 014037 (2020), arXiv:1911.03370 [hep-ph].
- [26] A. Kurkela and A. Mazeliauskas, Chemical equilibration in weakly coupled QCD, Phys. Rev. D 99, 054018 (2019), arXiv:1811.03068 [hep-ph].
- [27] X. Du and S. Schlichting, Equilibration of weakly coupled QCD plasmas, Phys. Rev. D 104, 054011 (2021), arXiv:2012.09079 [hep-ph].
- [28] S. Borsanyi, Z. Fodor, C. Hoelbling, S. D. Katz, S. Krieg, and K. K. Szabo, Full result for the QCD equation of state with 2+1 flavors, Phys. Lett. B 730, 99 (2014), arXiv:1309.5258 [hep-lat].
- [29] A. Bazavov et al. (HotQCD), Equation of state in (2+1)-flavor QCD, Phys. Rev. D 90, 094503 (2014), arXiv:1407.6387 [hep-lat].
- [30] X. Du, Heavy quark drag and diffusion coefficients in the prehydrodynamic QCD plasma, Phys. Rev. C 109, 014901 (2024), arXiv:2306.02530 [hep-ph].
- [31] C. Andres, L. Apolinário, F. Dominguez, M. G. Martinez, and C. A. Salgado, Medium-induced radiation with vacuum propagation in the pre-hydrodynamics phase, JHEP 03, 189, arXiv:2211.10161 [hep-ph].
- [32] A. Kurkela and Y. Zhu, Isotropization and hydrodynamization in weakly coupled heavy-ion collisions, Phys.

- Rev. Lett. **115**, 182301 (2015), arXiv:1506.06647 [hep-ph].
- [33] A. Kurkela, A. Mazeliauskas, J.-F. Paquet, S. Schlichting, and D. Teaney, Effective kinetic description of event-by-event pre-equilibrium dynamics in high-energy heavy-ion collisions, Phys. Rev. C 99, 034910 (2019), arXiv:1805.00961 [hep-ph].
- [34] A. Kurkela and E. Lu, Approach to Equilibrium in Weakly Coupled Non-Abelian Plasmas, Phys. Rev. Lett. 113, 182301 (2014), arXiv:1405.6318 [hep-ph].
- [35] A. Kurkela, A. Mazeliauskas, J.-F. Paquet, S. Schlichting, and D. Teaney, Matching the Nonequilibrium Initial Stage of Heavy Ion Collisions to Hydrodynamics with QCD Kinetic Theory, Phys. Rev. Lett. 122, 122302 (2019), arXiv:1805.01604 [hep-ph].
- [36] G. Giacalone, A. Mazeliauskas, and S. Schlichting, Hydrodynamic attractors, initial state energy and particle production in relativistic nuclear collisions, Phys. Rev. Lett. 123, 262301 (2019), arXiv:1908.02866 [hep-ph].
- [37] P. Romatschke, Relativistic Fluid Dynamics Far From Local Equilibrium, Phys. Rev. Lett. 120, 012301 (2018), arXiv:1704.08699 [hep-th].
- [38] G. Beuf, M. P. Heller, R. A. Janik, and R. Peschanski, Boost-invariant early time dynamics from AdS/CFT, JHEP 10, 043, arXiv:0906.4423 [hep-th].
- [39] S. Schlichting, New theoretical developments on the early-time dynamics and approach to equilibrium in Heavy-Ion collisions, EPJ Web Conf. 296, 01020 (2024), arXiv:2401.03841 [hep-ph].
- [40] X. Du, M. P. Heller, S. Schlichting, and V. Svensson, Exponential approach to the hydrodynamic attractor in Yang-Mills kinetic theory, Phys. Rev. D 106, 014016 (2022), arXiv:2203.16549 [hep-ph].
- [41] P. Romatschke and M. Strickland, Collective modes of an anisotropic quark gluon plasma, Phys. Rev. D 68, 036004 (2003), arXiv:hep-ph/0304092.
- [42] G. Nijs, W. van der Schee, U. Gürsoy, and R. Snellings, Transverse Momentum Differential Global Analysis of Heavy-Ion Collisions, Phys. Rev. Lett. 126, 202301 (2021), arXiv:2010.15130 [nucl-th].
- [43] G. Giacalone, G. Nijs, and W. van der Schee, Determination of the Neutron Skin of Pb208 from Ultrarelativistic Nuclear Collisions, Phys. Rev. Lett. 131, 202302 (2023), arXiv:2305.00015 [nucl-th].
- [44] K. J. Eskola, P. Paakkinen, H. Paukkunen, and C. A. Sal-gado, EPPS16: Nuclear parton distributions with LHC data, Eur. Phys. J. C 77, 163 (2017), arXiv:1612.05741 [hep-ph].
- [45] S. Camarda et al., DYTurbo: Fast predictions for Drell-Yan processes, Eur. Phys. J. C 80, 251 (2020), [Erratum: Eur.Phys.J.C 80, 440 (2020)], arXiv:1910.07049 [hep-ph].

- [46] S. Endres, H. van Hees, J. Weil, and M. Bleicher, Coarse-graining approach for dilepton production at energies available at the CERN Super Proton Synchrotron, Phys. Rev. C 91, 054911 (2015), arXiv:1412.1965 [nucl-th].
- [47] S. Endres, H. van Hees, and M. Bleicher, Probing the QCD phase diagram with dileptons - a study using coarse-grained transport dynamics, Acta Phys. Polon. Supp. 10, 549 (2017), arXiv:1609.09140 [nucl-th].
- [48] J. Berges, K. Reygers, N. Tanji, and R. Venugopalan, Parametric estimate of the relative photon yields from the glasma and the quark-gluon plasma in heavy-ion collisions, Phys. Rev. C 95, 054904 (2017), arXiv:1701.05064 [nucl-th].
- [49] A. Monnai, Prompt, pre-equilibrium, and thermal photons in relativistic nuclear collisions, J. Phys. G 47, 075105 (2020), arXiv:1907.09266 [nucl-th].
- [50] O. Garcia-Montero, N. Löher, A. Mazeliauskas, J. Berges, and K. Reygers, Probing the evolution of heavy-ion collisions using direct photon interferometry, Phys. Rev. C 102, 024915 (2020), arXiv:1909.12246 [hepph].
- [51] O. Garcia-Montero, Non-equilibrium photons from the bottom-up thermalization scenario, Annals Phys. 443, 168984 (2022), arXiv:1909.12294 [hep-ph].
- [52] X.-Y. Wu, L. Du, C. Gale, and S. Jeon, Probing the equilibration of the QCD matter created in heavy-ion collisions with dileptons, (2024), arXiv:2407.04156 [nuclth].
- [53] A. Kurkela and A. Mazeliauskas, Chemical Equilibration in Hadronic Collisions, Phys. Rev. Lett. 122, 142301 (2019), arXiv:1811.03040 [hep-ph].
- [54] Kømpøst, https://github.com/KMPST/KoMPoST [Accessed: 2023-08-17)].
- [55] J. Uphoff, O. Fochler, Z. Xu, and C. Greiner, Heavy quark production at RHIC and LHC within a partonic transport model, Phys. Rev. C 82, 044906 (2010), arXiv:1003.4200 [hep-ph].
- [56] B.-W. Zhang, C.-M. Ko, and W. Liu, Thermal charm production in a quark-gluon plasma in Pb-Pb collisions at $s^{**}(1/2)(NN) = 5.5$ -TeV, Phys. Rev. C **77**, 024901 (2008), arXiv:0709.1684 [nucl-th].
- [57] K. Zhou, Z. Chen, C. Greiner, and P. Zhuang, Thermal Charm and Charmonium Production in Quark Gluon Plasma, Phys. Lett. B 758, 434 (2016), arXiv:1602.01667 [hep-ph].
- [58] K. Boguslavski, A. Kurkela, T. Lappi, and J. Peuron, Heavy quark diffusion in an overoccupied gluon plasma, JHEP 09, 077, arXiv:2005.02418 [hep-ph].
- [59] F. Zhou, J. Brewer, and A. Mazeliauskas, Minijet quenching in non-equilibrium quark-gluon plasma, (2024), arXiv:2402.09298 [hep-ph].